Broadband Overlaid Inset Dielectric Guide Coupler with Very Flat Coupling

Z. Fan, *Member, IEEE*, and Y. M. M. Antar, *Senior Member, IEEE*

Abstract— **In this paper overlaid parallel coupled inset dielectric guides are proposed for broadband applications to directional couplers. This structure provides much flatter and higher coupling than the conventional one without an overlay. The propagation and coupling characteristics of the coupled guides are obtained by using the integral equation formulation and Galerkin's procedure. Numerical results for two limiting cases are compared with available measured data, showing good agreement. Effects of thickness and dielectric constant of the overlay are examined on coupling and bandwidth. It is found that by suitable choice of these parameters very flat coupling can be achieved for a wide frequency range which is still within the fundamental-mode bandwidth. Examples of couplers with the bandwidth exceeding 45% for the coupling of 3 ± 0.25 dB are presented.**

I. Introduction

DUE TO several advantages of inset dielectric guides (IDG's) over image guides and microstrip lines, various IDG structures have recently been investigated both experimentally and theoretically, and some of their practical applications to microwave and millimeter-wave circuits and antennas have been demonstrated [1]–[4]. Studies of the aspect ratio and multilayer dielectric filling of the single IDG have shown that the one-layer structure can offer wider bandwidth than a rectangular waveguide and two-layer one may have very wide bandwidth exceeding that of a ridge waveguide [5]. It has been also demonstrated that optimum flat coupling between two parallel coupled IDG's exists for a certain value of the aspect ratio [6]. Using single and coupled IDG's, different components such as directional couplers have been developed and analyzed by using several rigorous full wave methods including the transverse resonance diffraction technique and spectral domain approach. Through combining the single IDG with microstrips, both strong and weak directional couplers have been realized [7]. Two parallel coupled IDG's can be also used to design directional couplers. Very low return loss and high isolation for this kind of couplers have been demonstrated experimentally, but the electromagnetic coupling has been found to change significantly with increasing frequency [8] [9]. To compensate for this frequency dependence, holes in the metal separation walls have been proposed to be used to introduce additional coupling mechanism [10]. However, the use of these holes increases the fabrication difficulty, and accurate modeling of the hole coupling is complicated.

Manuscript received December 12, 1995; revised July 22, 1996.

The authors are with the Department of Electrical and Computer Engineering, Royal Military College of Canada, Kingston, ON K7K 5L0, Canada.

Publisher Item Identifier S 0018-9480(96)07918-5.

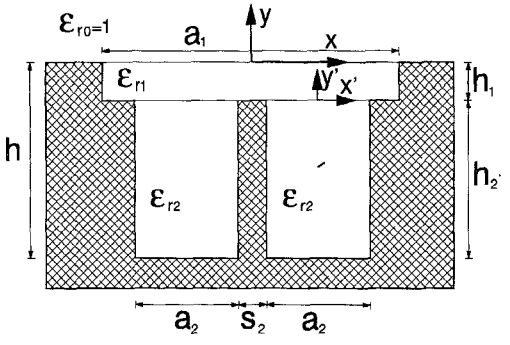

Fig. 1. Cross section of the overlaid parallel coupled inset dielectric guides and coordinate systems used in the analysis.

In this paper, the use of a dielectric layer over the parallel coupled IDG's is proposed to increase the coupling and to achieve very wide band for the flat coupling. This new structure as shown in Fig. 1 can be viewed as a modification of conventional coupled IDG's by reducing the height of a metal separation wall for the case of $a_1 = 2a_2 + s_2$. With reducing the height, the interaction between guides becomes stronger, and therefore the coupling is increased, resulting in a shorter section length for 3 dB coupling which is desirable for the design of small circuits. Further, the coupling becomes much flatter over a wide bandwidth. With their potential applications for wideband flat coupling, the overlaid parallel coupled IDG's are analyzed here by using a rigorous full-wave method based on the integral equation formulation and Galerkin's procedure. Numerical results for various structural and material parameters are presented, and effects of the overlay on the propagation and coupling characteristics are illustrated.

II. Analysis

Fig. 1 illustrates the cross-sectional view of the overlaid parallel coupled inset dielectric guides and two coordinate systems to be used in the analysis. In the following analysis, time and z dependence $e^{j(\omega t-\beta z)}$ will be omitted for the sake of brevity, where β is the propagation constant. Integral equations for tangential electric field components at two apertures are first obtained by using Fourier transforms and then solved for propagation constants by employing Galerkin's method. Finally, the simple expressions for scattering parameters are given.

Due to the symmetry of the structure with respect to the $x = 0$ plane, the structure is capable of supporting both

0018–9480/96$05.00 © 1996 IEEE

odd and even modes, and hence only the right-hand half of the cross section need to be considered for the analysis. By definition, the mode is called odd when E_z is an odd function of x and the mode is called even when E_z is an even function of x. Electromagnetic field components can be represented through their Fourier transforms.

For the air region

$$E_y(x,y) = \frac{1}{2\pi}\int_{-\infty}^{\infty} \tilde{E}_y(\alpha_0, y)e^{-j\alpha_0 x}\, d\alpha_0 \tag{1}$$

For the overlay region

$$E_y(x,y) = \frac{1}{a_1}\sum_{n=-\infty}^{\infty} \tilde{E}_y(\alpha_{1n}, y)e^{-j\alpha_{1n}x} \tag{2}$$

For the right-hand groove region

$$\begin{aligned} E_y(x',y) &= \frac{1}{a_2}\sum_{n=-\infty}^{\infty} \tilde{E}_y(\alpha_{2n}, y)e^{-j\alpha_{2n}x'} \\ &= \frac{1}{a_2}\sum_{n=-\infty}^{\infty} \tilde{E}_y(\alpha^o_{2n}, y)e^{-j\alpha^o_{2n}x'} \\ &\quad + \frac{1}{a_2}\sum_{n=-\infty}^{\infty} \tilde{E}_y(\alpha^e_{2n}, y)e^{-j\alpha^e_{2n}x'} \end{aligned} \tag{3}$$

and similarly for other field components. In the above equations, the tilde ˜ denotes Fourier-transformed components. Discrete transform variables α_{1n} and α_{2n} are determined satisfying the electric field boundary conditions on the sidewalls of the overlay and the right-hand groove. $\alpha_{1n} = 2n\pi/a_1, (2n+1)\pi/a_1$ $(n = 0, \pm1, \pm2, \cdots)$ for the E_z odd and even modes, respectively. $\alpha_{2n} = n\pi/a_2$, which is divided into two parts: $\alpha^o_{2n} = 2n\pi/a_2$ and $\alpha^e_{2n} = (2n+1)\pi/a_2$. The superscript o denotes one part of the fields inside the right-hand groove with the tangential electrical field components E^o_z and E^o_x being odd and even functions of x' respectively; e stands for the other part with E^e_z and E^e_x being even and odd functions of x' respectively.

The wave equations in the Fourier transform domain are now solved in each region with the application of the boundary condition at the base of the right-hand groove and the radiation condition at infinity. The modal amplitude coefficients in each region are then obtained in terms of the tangential electrical field components E^a_x, E^a_z at the $y = 0$ interface and $E^b_x = E^o_x + E^e_x, E^b_z = E^o_z + E^e_z$ at the $y = -h_1$ interface. Next, the relations between tangential magnetic and electric field components at these two interfaces are obtained, and can be expressed in the following matrix form

$$\begin{bmatrix} -\tilde{H}_z(\alpha_0, 0^+) \\ +\tilde{H}_x(\alpha_0, 0^+) \end{bmatrix} = [P_0(\alpha_0)] \begin{bmatrix} \tilde{E}^a_x(\alpha_0) \\ \tilde{E}^a_z(\alpha_0) \end{bmatrix} \tag{4}$$

$$\begin{bmatrix} +\tilde{H}_z(\alpha_{1n}, 0^-) \\ -\tilde{H}_x(\alpha_{1n}, 0^-) \\ -\tilde{H}_z(\alpha_{1n}, -h_1^+) \\ +\tilde{H}_x(\alpha_{1n}, -h_1^+) \end{bmatrix} = \begin{bmatrix} P_1(\alpha_{1n}) & R_1(\alpha_{1n}) \\ R_1(\alpha_{1n}) & P_1(\alpha_{1n}) \end{bmatrix} \cdot \begin{bmatrix} \tilde{E}^a_x(\alpha_{1n}) \\ \tilde{E}^a_z(\alpha_{1n}) \\ \tilde{E}^b_x(\alpha_{1n}) \\ \tilde{E}^b_z(\alpha_{1n}) \end{bmatrix} \tag{5}$$

$$\begin{bmatrix} +\tilde{H}^{o,e}_z(\alpha^{o,e}_{2n}, -h_1^-) \\ -\tilde{H}^{o,e}_{x'}(\alpha^{o,e}_{2n}, -h_1^-) \end{bmatrix} = [P_2(\alpha^{o,e}_{2n})] \begin{bmatrix} \tilde{E}^{o,e}_{x'}(\alpha^{o,e}_{2n}) \\ \tilde{E}^{o,e}_z(\alpha^{o,e}_{2n}) \end{bmatrix} \tag{6}$$

where the Fourier transformed Green's functions $[P_i]$ and $[R_i]$ $(i = 0, 1, 2)$ are 2×2 matrices, and are given in the Appendix. For the E_z odd modes

$$\begin{aligned} \tilde{E}^b_{x,z}(\alpha_{1n}) &= 2\cos\frac{\alpha_{1n}(s_2+a_2)}{2}\tilde{E}^o_{x',z}(\alpha_{1n}) \\ &\quad + 2j\sin\frac{\alpha_{1n}(s_2+a_2)}{2}\tilde{E}_{x',z}{}^e(\alpha_{1n}). \end{aligned} \tag{7}$$

For the E_z even modes, cos and j sin in the above equation are replaced by j sin and cos . The Fourier transforms of tangential electric field components at these two interfaces are obtained as follows:

$$\tilde{E}^a_x(\alpha_{1n}) = \int_{-(a_1/2)}^{a_1/2} E^a_x(x)e^{j\alpha_{1n}x}\, dx \tag{8}$$

$$\tilde{E}^a_z(\alpha_{1n}) = \frac{j}{\alpha_{1n}}\int_{-(a_1/2)}^{a_1/2} \frac{\partial E^a_z(x)}{\partial x}e^{j\alpha_{1n}x}\, dx \tag{9}$$

$$\tilde{E}^{o,e}_{x'}(\alpha^{o,e}_{2n}) = \int_{-(a_2/2)}^{a_2/2} E^{o,e}_{x'}(x')e^{j\alpha^{o,e}_{2n}x'}\, dx' \tag{10}$$

$$\tilde{E}^{o,e}_z(\alpha^{o,e}_{2n}) = \frac{j}{\alpha^{o,e}_{2n}}\int_{-(a_2/2)}^{a_2/2} \frac{\partial E^{o,e}_z(x')}{\partial x'}e^{j\alpha^{o,e}_{2n}x'}\, dx'. \tag{11}$$

Note that $\partial E^a_z(x)/\partial x$ and $\partial E^{o,e}_z(x')/\partial x'$ are used instead of $E^a_z(x)$ and $E^{o,e}_z(x')$ because they satisfy the same boundary and singular edge conditions as $E^a_x(x)$ and $E^{o,e}_{x'}(x')$, respectively. As a result, in the Galerkin's procedure the basis functions for $\partial E^a_z(x)/\partial x$ and $\partial E^{o,e}_z(x')/\partial x'$ can be chosen to be the same as those for $E^a_x(x)$ and $E^{o,e}_{x'}(x')$, respectively.

Transforming (4), (5), and (6) into the spatial domain, and applying the continuous conditions for the tangential magnetic field components at the $y = 0$ and $y = -h_1$ interfaces, we can obtain the following integral equations

$$\begin{aligned} &\frac{1}{2\pi}\int_{-\infty}^{\infty} \begin{bmatrix} P_0 & 0 \\ 0 & 0 \end{bmatrix} \begin{bmatrix} \tilde{E}^a_x(\alpha_0) \\ \tilde{E}^a_z(\alpha_0) \\ 0 \\ 0 \end{bmatrix} e^{-j\alpha_0 x}\, d\alpha_0 \\ &\quad + \frac{1}{a_1}\sum_{n=-\infty}^{\infty} \begin{bmatrix} P_1 & R_1 \\ R_1 & P_1 \end{bmatrix} \begin{bmatrix} \tilde{E}^a_x(\alpha_{1n}) \\ \tilde{E}^a_z(\alpha_{1n}) \\ \tilde{E}^b_x(\alpha_{1n}) \\ \tilde{E}^b_z(\alpha_{1n}) \end{bmatrix} e^{-j\alpha_{1n}x} \\ &\quad + \frac{1}{a_2}\sum_{n=-\infty}^{\infty} \begin{bmatrix} 0 & 0 \\ 0 & P_2 \end{bmatrix} \begin{bmatrix} 0 \\ 0 \\ \tilde{E}^o_{x'}(\alpha^o_{2n}) \\ \tilde{E}^o_z(\alpha^o_{2n}) \end{bmatrix} e^{-j\alpha^o_{2n}x'} \\ &\quad + \frac{1}{a_2}\sum_{n=-\infty}^{\infty} \begin{bmatrix} 0 & 0 \\ 0 & P_2 \end{bmatrix} \begin{bmatrix} 0 \\ 0 \\ \tilde{E}^e_{x'}(\alpha^e_{2n}) \\ \tilde{E}^e_z(\alpha^e_{2n}) \end{bmatrix} e^{-j\alpha^e_{2n}x'} = 0 \end{aligned} \tag{12}$$

Integral equations in (12) are solved for the propagation constants of discrete modes by applying Galerkin's procedure, where $E^a_x(x)$ and $E^{o,e}_{x'}(x')$ are expanded in terms of basis functions. Here Gegenbauer polynomials are chosen as basis

functions since their weight function fits the singularity of order $r^{-(1/3)}$ at the rectangular metal corners, as discussed in [1].

Since there are two parallel grooves coupled tightly by connection with an overlay, there exists a certain frequency range over which only the first E_z even and odd modes can propagate. In this range the characteristics of these two modes can be used to realize a directional coupler, where the coupling occurs in the "forward direction. For this coupler with length of L, the transmission and coupling coefficients can be obtained from the difference between the propagation constant β_e of the dominant even mode and that β_o of odd mode [11]

$$|S_{21}| = \left|\cos\left(\frac{\beta_e - \beta_o}{2}L\right)\right| \tag{13}$$

$$|S_{31}| = \left|\sin\left(\frac{\beta_e - \beta_o}{2}L\right)\right|. \tag{14}$$

The coupling length for a 3-dB directional coupler $L_{3\text{dB}}$ is given by $\pi/2(\beta_e - \beta_o)$.

III. Results

The convergence of solutions for propagation constants has been tested with different number of basis functions. It has been found that five basis functions for $E^a_{x,z}$ and three for $E^{e,o}_{x,z}$ can be used to achieve accurate solutions for propagation constants of both E_z even and odd modes to five significant digits, and for their difference to three significant digits for all the structural parameters used in this paper. To verify the accuracy of the analysis presented in the previous section, computed results for two special cases where h_1 or h_2 approaches zero are compared with measured data available in the literature. When h_1 approaches zero, the overlaid coupled IDG's are reduced to the conventional coupled IDG's, propagation constants and coupling coefficient of which were measured and reported in [8] and [9]. Comparison of our computed results with these measured data is shown in Fig. 2. Clearly, very good agreement is obtained for propagation constants of the dominant E_z even and odd modes. There is also reasonable agreement for the coupling coefficient. When h_2 approaches zero, the overlaid coupled IDG's are reduced to a single IDG. Propagation constants of the first even and odd modes for this single guide were measured and reported in [5]. In Fig. 3, these measured data are compared with our computed results for this limiting case. Again, good agreement is obtained for the propagation constants.

Effects of variation in the value of the height h_1 of the overlay on propagation and coupling characteristics are investigated first. Fig. 4 shows normalized propagation constants of the dominant E_z even and odd modes for different values of h_1. During the frequency range shown here, as h_1 increases, normalized propagation constant of the dominant even mode increases. On the contrary, the effect of changing h_1 on the dominant odd mode is very small. This may be explained by the the fact that the $x = 0$ plane is a magnetic or electric wall for the E_z even and odd modes, respectively. As expected, when h_1 increases, the difference between propagation constants of the dominant E_z even and odd modes increases due

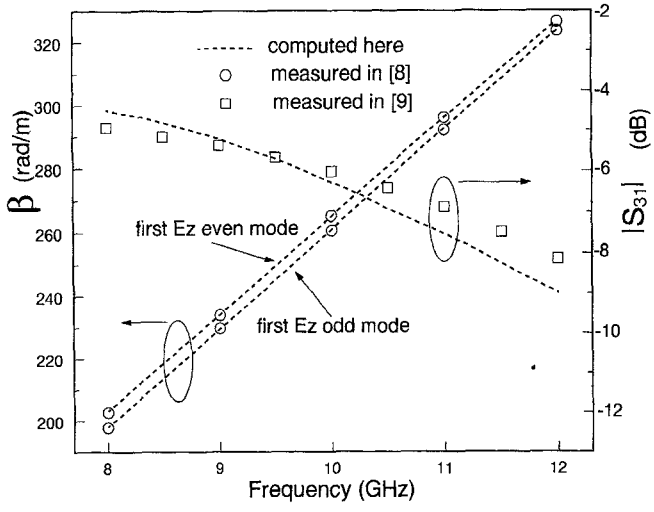

Fig. 2. Comparison of propagation constants for the dominant E_z even and odd modes and their coupling coefficient of the 250 mm coupled IDG section with the measured data reported in [8] and [9] for the case where h_1 approaches zero. ($a_1 = 22.02$ mm, $\varepsilon_{r1} = \varepsilon_{r2} = 2.04, a_2 = 10.16$ mm, $h = 15.24$ mm, $s_2 = 1\ 7$ mm).

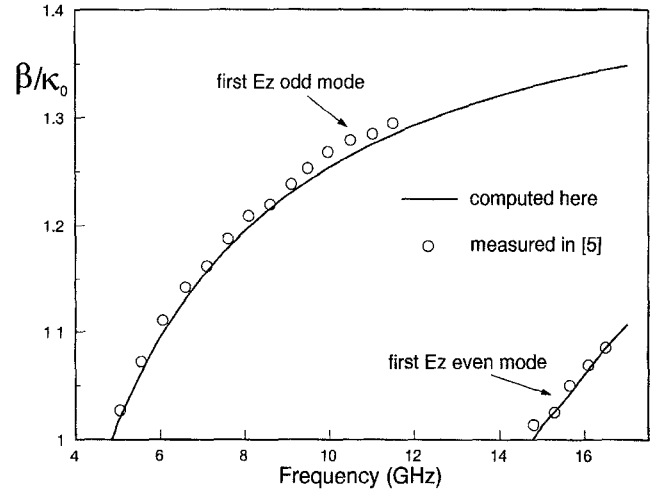

Fig. 3. Comparison of normalized propagation constants for the first E_z even and odd modes of the coupled IDG with the measured data reported in [5] for the case where h_2 approaches zero. ($a_1 = 10.16$ mm, $\varepsilon_{r1} = \varepsilon_{r2} = 2.04, a_2 = 4.58$ mm, $h = 15.24$ mm, $s_2 = 1.0$ mm).

to more interaction between these two guides. As a result, the coupling increases and hence the length required for the 3 dB coupling is reduced. This can clearly be observed in Fig. 5, which shows difference between the propagation constants of the dominant E_z even and odd modes and length for the 3-dB coupling as a function of frequency for different values of h_1. It is more interesting to note that as h_1 increases, the difference between the propagation constants of the dominant E_z even and odd modes becomes flatter over this frequency range. This results in flatter coupling. To clearly illustrate this, in Fig. 6 coupling coefficient $|S_{31}|$ of the dominant E_z even and odd modes of the coupled IDG section is shown as a function of frequency for different values of h_1. For $h_1 = 0.1$ mm, The coupling $|S_{31}|$ changes rapidly as frequency increases. In fact, the coupling at lower end of the frequency range is about 3.5 dB higher than that at higher end. However, as h_1

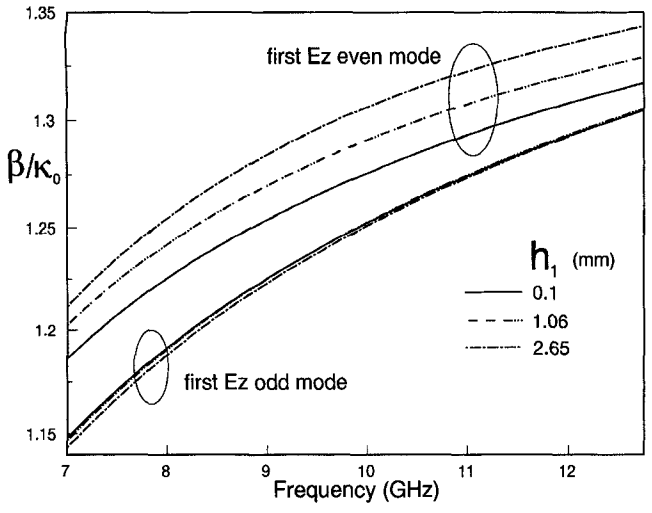

Fig. 4. Normalized propagation constants of the dominant E_z even and odd modes as a function of frequency for different values of h_1 ($a_1 = 16.02$ mm, $\varepsilon_{r1} = \varepsilon_{r2} = 2.04, a_2 = 7.16$ mm, $h = 15.24$ mm, $s_2 = 1.7$ mm).

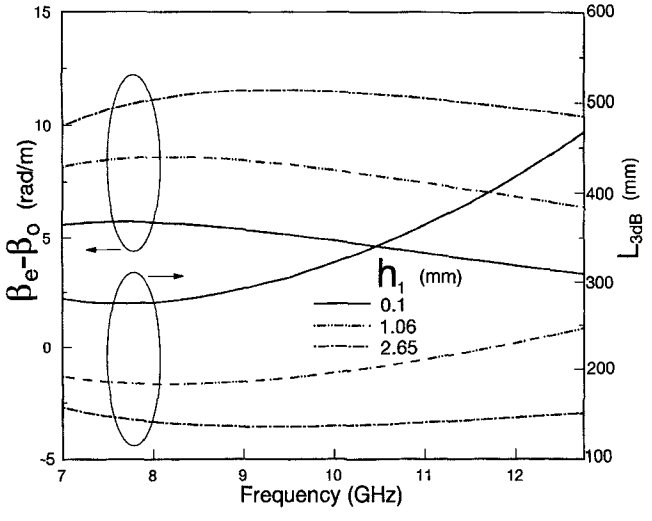

Fig. 5. Difference between the propagation constants of the dominant E_z even and odd modes and length for the 3-dB coupling as a function of frequency for different values of h_1 ($a_1 = 16.02$ mm, $\varepsilon_{r1} = \varepsilon_{r2} = 2.04, a_2 = 7.16$ mm, $h = 15.24$ mm, $s_2 = 1.7$ mm).

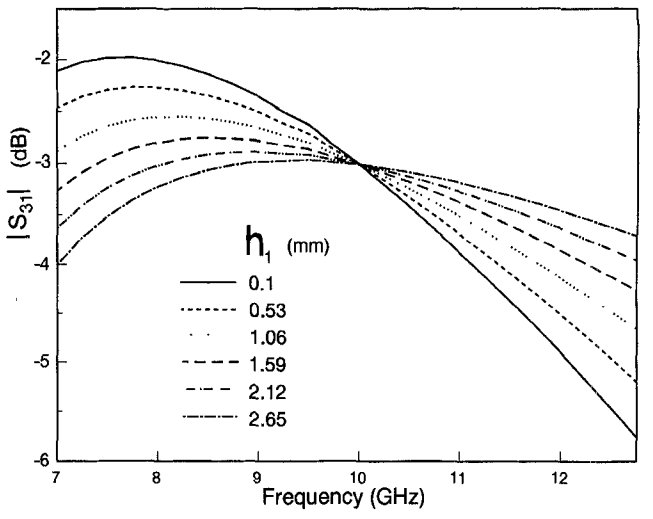

Fig. 6. Coupling coefficient of the dominant E_z even and odd modes of the coupled IDG section as a function of frequency for different values of h_1 ($a_1 = 16.02$ mm, $\varepsilon_{r1} = \varepsilon_{r2} = 2.04, a_2 = 7.16$ mm, $h = 15.24$ mm, $s_2 = 1.7$ mm, $L = L_{3dB}$ at 10 GHz).

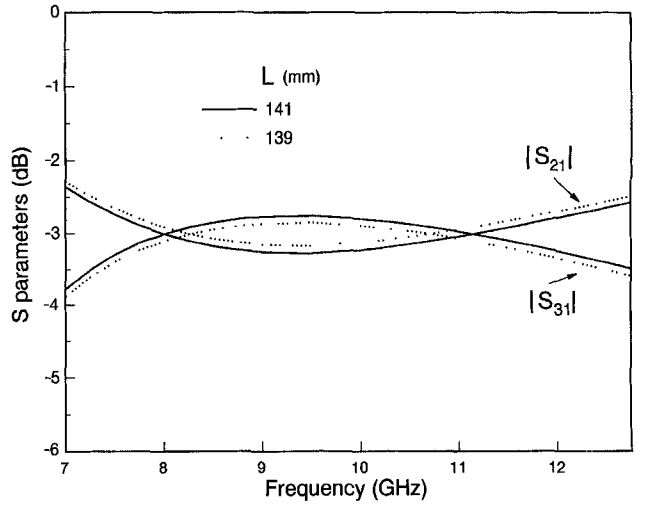

Fig. 7. Scattering characteristics of the dominant E_z even and odd modes of the coupled IDG section as a function of frequency for $h_1 = 2.65$ mm ($a_1 = 16.02$ mm, $\varepsilon_{r1} = \varepsilon_{r2} = 2.04, a_2 = 7.16$ mm, $h = 15.24$ mm, $s_2 = 1.7$ mm).

increases up to 2.65 mm, the coupling decreases at the lower end and increases at the higher end, respectively. Therefore flatter coupling is achieved. Fig. 7 shows scattering parameters of the dominant E_z even and odd modes of the coupled IDG section as a function of frequency for $h_1 = 2.65$ mm. It can be seen that the flat coupling is obtained for a wide range of frequency. For $L = 139$ and 141 mm, we can obtain the bandwidth of 35% (from 7.93 to 11.33 GHz) and 46% (from 7.55 to 12.05 GHz) for the coupling variation of ± 0.15 dB and ± 0.25 dB, respectively. It is also important to note that for that bandwidth, all the higher order modes are cut off, as seen from Fig. 8 which shows normalized propagation constants of the first and second E_z even and odd modes as a function of frequency for two different values of h_1. When h_1 is increased to be higher than 2.65 mm, further improvement in the coupling flatness will be achieved, but the second E_z even mode will begin to appear in the above-mentioned latter band. It has been found that if the width a_2 of each guide is reduced, the cutoff frequency of the second E_z even mode gets higher, resulting in the wider fundamental-mode bandwidth. Therefore, by further increasing h_1 along with the reduction in a_2, the useable bandwidth for the 3 ± 0.15 dB or 3 ± 0.25 dB coupling, during which only first E_z even and odd modes can propagate, will be further increased. In comparison to the directly connected image guides, this overlaid coupled IDG's offer wider band for the flat coupling, but without the propagation of higher-order modes during the band. In [12], directly connected image guides were studied for flat coupling, the bandwidth of as high as 28% for the 3 ± 0.25 dB coupling was achieved, but the first higher-order mode can propagate in this band.

Effects of changing the dielectric constant ε_{r1} of the overlay are also investigated. Fig. 9 shows difference between the

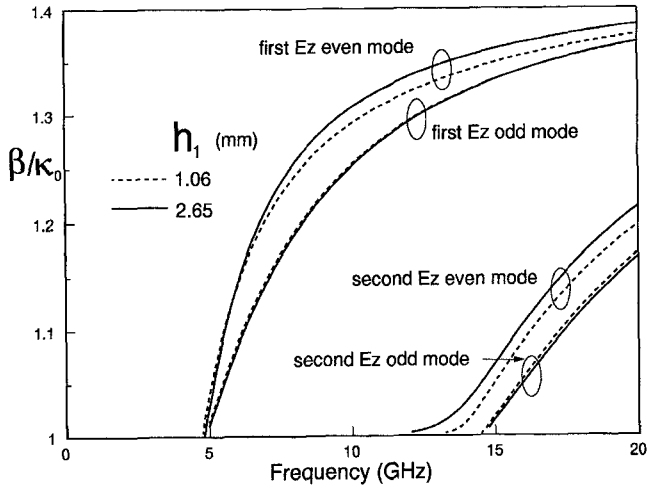

Fig. 8. Normalized propagation constants of the first and second E_z even and odd modes as a function of frequency for different values of h_1 ($a_1 = 16.02$ mm, $\varepsilon_{r1} = \varepsilon_{r2} = 2.04, a_2 = 7.16$ mm, $h = 15.24$ mm, $s_2 = 1.7$ mm).

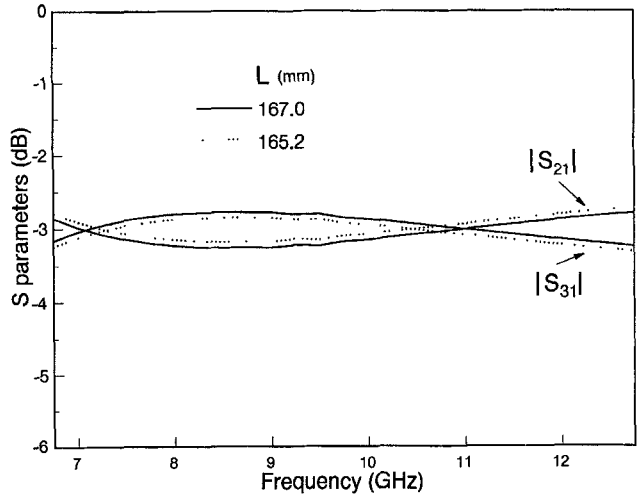

Fig. 10. Scattering characteristics of the dominant E_z even and odd modes of the coupled IDG section as a function of frequency for $\varepsilon_{r1} = 6.0$ ($a_1 = 16.02$ mm, $h_1 = 0.53$ mm, $\varepsilon_{r2} = 2.04, a_2 = 7.16$ mm, $h_2 = 14.71$ mm, $s_2 = 1.7$ mm).

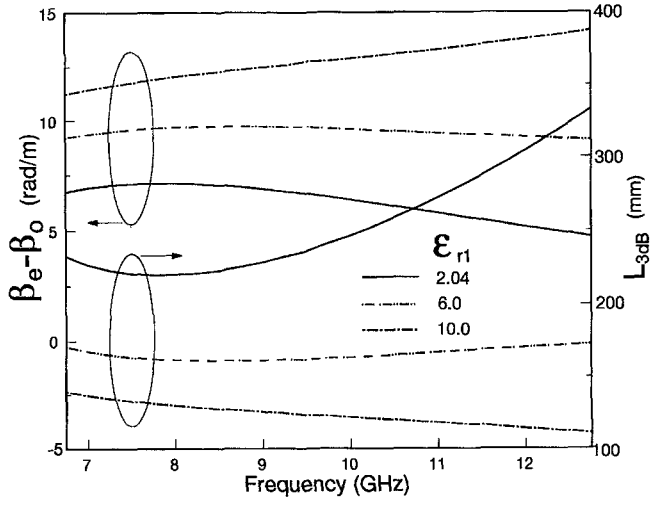

Fig. 9. Difference between the propagation constants of the dominant E_z even and odd modes and length for the 3-dB coupling as a function of frequency for different values of ε_{r1} ($a_1 = 16.02$ mm, $h_1 = 0.53$ mm, $\varepsilon_{r2} = 2.04, a_2 = 7.16$ mm, $h_2 = 14.71$ mm, $s_2 = 1.7$ mm).

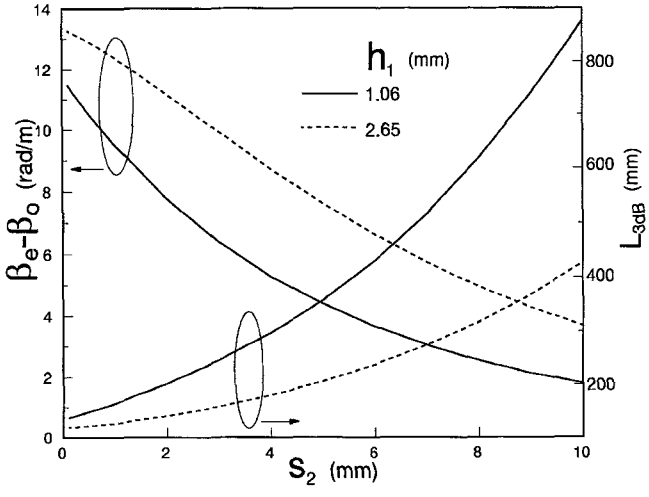

Fig. 11. Difference between the propagation constants of the dominant E_z even and odd modes and length for the 3-dB coupling as a function of s_2 for different values of h_1 ($\varepsilon_{r1} = \varepsilon_{r2} = 2.04, a_2 = 7.16$ mm, $h = 15.24$ mm, $a_1 = 2a_2 + s_2, f = 9.5$ GHz).

propagation constants of the dominant E_z even and odd modes and length for the 3-dB coupling for different values of ε_{r1}. As ε_{r1} increases, the difference increases, and hence due to stronger coupling the length for 3 dB coupling decreases. When ε_{r1} is small, the difference decreases with increasing frequency. But, when ε_{r1} is large, the difference increases with increasing frequency. Therefore, with suitable choice of ε_{r1}, very flat coupling can be achieved. In fact, the curve for $\varepsilon_{r1} = 6.0$ is seen to be very flat. Fig. 10 shows scattering characteristics of the dominant E_z even and odd modes of the coupled IDG section as a function of frequency for $\varepsilon_{r1} = 6.0$. For $L = 165.2$ mm, we can obtain the bandwidth of 49% (from 7.0 to 11.5 GHz) for the coupling variation of ± 0.15 dB. For $L = 167.0$ mm, the bandwidth of as high as 62% (from 6.7 to 12.75 GHz) can be achieved within the tolerance of ± 0.25 dB from the 3 dB coupling.

From a practical viewpoint, choice of the width s_2 of the metal separation wall is also important to achieve the required coupling for a specified length. Fig. 11 shows the difference between the propagation constants of the dominant E_z even and odd modes and length for the 3-dB coupling as a function of s_2. As s_2 increases, the difference decreases because the fields decay from the center of each guide. As a result, the length for 3 dB coupling increases. To obtain high coupling for a small guide section, s_2 should be chosen to be as small as possible in the actual implementation.

IV. Conclusion

The overlaid parallel coupled IDG's have been proposed in order to reduce the coupler length for the 3 dB coupling and to flatten the coupling over a wide frequency range. The integral equation formulation and Galerkin's procedure have been used to analyze the characteristics of this structure. Good convergence for propagation constants have been demonstrated and the accuracy of the analysis has been verified

by comparison with available experimental results for two limiting cases. Numerical results for propagation and coupling characteristics have been presented for various structural and material parameters. As the thickness and dielectric constant of the overlay increase, the coupling increases due to stronger interaction between two parallel guides, however the cutoff frequency of the first higher-order mode decreases. It has been found that there are optimum values of these two parameters for the maximum useable bandwidth, during which a certain tolerance limit for the coupling is met and only first E_z even and odd modes can propagate. The bandwidth for two examples has been shown to exceed 45% under the tolerance limit of ± 0.25 dB of deviation in coupling from 3 dB. The new guide coupler with broadband flat coupling characteristics should be very useful for microwave and millimeter-wave integrated circuits.

APPENDIX

The quantities in (4), (5), and (6) are given by

$$[P_i] = \frac{1}{\alpha_{\text{in}}^2 + \beta^2} \begin{bmatrix} \beta^2 C_i - \alpha_{\text{in}}^2 D_i & -\alpha_{\text{in}}\beta(C_i + D_i) \\ -\alpha_{\text{in}}\beta(C_i + D_i) & \alpha_{\text{in}}^2 C_i - \beta^2 D_i \end{bmatrix} \tag{15}$$

$$[R_i] = \frac{-1}{\cosh(\gamma_i h_i)}[P_i] \tag{16}$$

where $i = 0, 1, 2$, and

$$C_i = \frac{-j\gamma_i}{\omega\mu_0 \tanh(\gamma_i h_i)} \tag{17}$$

$$D_i = \frac{-j\omega\varepsilon_0\varepsilon_{ri}}{\gamma_i \tanh(\gamma_i h_i)} \tag{18}$$

$$\gamma_i^2 = \alpha_{\text{in}}^2 + \beta^2 - \omega^2\mu_0\varepsilon_0\varepsilon_{ri}. \tag{19}$$

Note that when $i = 0$ for the air region, $\tanh(\gamma_0 h_0)$ and $\cosh(\gamma_0 h_0)$ are replaced by 1.

REFERENCES

[1] T. Rozzi and S. J. Hedges, "Rigorous analysis and network modeling of the inset dielectric guide," *IEEE Trans. Microwave Theory Tech.*, vol. MTT-35, pp. 823–833, Sept. 1987.

[2] T. Rozzi, A. Morini and G. Gerini, "Analysis and applications of microstrip loaded inset dielectric waveguide," *IEEE Trans. Microwave Theory Tech.*, vol. 40, pp. 272–278, Feb. 1992.

[3] N. Izzat, S.R. Pennock and T. Rozzi, "Space domain analysis of micro-IDG structures," *IEEE Trans. Microwave Theory Tech.*, vol. 42, pp. 1074–1078, June 1994.

[4] L. Ma, T. Rozzi and S. R. Pennock, "Design of multiple array flat millimetric antennas in IDG," in *Proc. 21th European Microwave Conf.*, 1991, pp. 641–646.

[5] S. R. Pennock, N. Izzat and T. Rozzi, "Very wideband operation of twin-layer inset dielectric guide," *IEEE Trans. Microwave Theory Tech.*, vol. 40, pp. 1910–1917, Oct. 1992.

[6] Z. Fan and S. R. Pennock, "Hybrid mode analysis of parallel coupled inset dielectric guides," *IEE Proc.—Microw. Antenna Propag.*, vol. 42, pp. 57–62, Feb. 1995.

[7] ——, "Broadside coupled strip inset dielectric guide and its directional coupler application," *IEEE Trans. Microwave Theory Tech.*, vol. 43, pp. 612–619, Mar. 1995.

[8] S. R. Pennock, D. M. Boskovic and T. Rozzi, "Analysis of coupled inset dielectric guides under LSE and LSM polarization," *IEEE Trans. Microwave Theory Tech.*, vol. 40, pp. 916–924, May 1992.

[9] T. Rozzi, S. R. Pennock and D. Boskovic, "Dispersion characteristic of coupled inset dielectric guide," in *Proc. 20th European Microwave Conf.*, 1990, pp. 1175–1180.

[10] S. R. Pennock, D. Boskovic and T. Rozzi, "Broadband inset dielectric guide coupler," in *Proc. 21th European Microwave Conf.*, 1991, pp. 1142–1147.

[11] J. Miao and T. Itoh, "Hollow image guide and overlayed image guide coupler," *IEEE Trans. Microwave Theory Tech.*, vol. MTT-30, pp. 1826–1831, Nov. 1982.

[12] D. I. Kim, D. Kawabe, K. Araki and Y. Naito, "Directly connected image guide 3-dB couplers with very flat couplings," *IEEE Trans. Microwave Theory Tech.*, vol. MTT-32, pp. 621–627, June 1984.

Z. Fan (S'92–M'96) received the B.Sc degree in physics from Hubei University, P.R. China, in 1983, and the M.Sc. degree in microwave and antennas from Wuhan University, P.R. China in 1986. In 1994 he received the Ph.D. degree from the University of Bath, U.K. for his work on inset dielectric guide structures and ferrite loaded finlines.

From 1986 to 1991 he was a Teaching Assistant and then a Lecturer at Wuhan University. From 1991 to 1994 he was a postgraduate student at the University of Bath. Since January 1995, he has been a Research Associate at Royal Military College of Canada. His research interests are in the areas of novel waveguide structures, microstrip patch antennas and dielectric resonator antennas, ferrite devices, and microwave circuits.

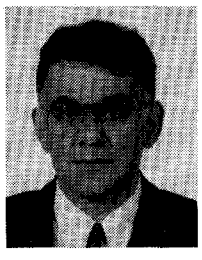

Y. M. M. Antar (S'73–M'76–SM'85) was born on November 18, 1946, in Meit Temmama, Egypt. He received the B.Sc. (Hons.) degree in 1966 from Alexandria University, Egypt, and the M.Sc. and Ph.D. degrees from the University of Manitoba, Winnipeg, Canada, in 1971 and 1975, respectively, all in electrical engineering.

In 1966, he joined the Faculty of Engineering at Alexandria, where he was involved in teaching and research. At the University of Manitoba he held a University Fellowship, an NRC Postgraduate and Postdoctoral Fellowships. From 1976 to 1977 he was with the Faculty of Engineering at the University of Regina. In June 1977, he was awarded a Visiting Fellowship from the Government of Canada to work at the Communications Research Centre of the Department of Communications, Shirley's Bay, Ottawa, where he was involved in research and development of satellite technology with the Space Electronics group. In May 1979, he joined the Division of Electrical Engineering, National Research Council of Canada, Ottawa, where he worked on polarization radar applications in remote sensing of precipitation, radio wave propagation, electromagnetic scattering and radar cross section investigations. In November 1987, he joined the staff of the Department of Electrical and Computer Engineering at the Royal Military College of Canada in Kingston, where he is now professor of Electrical Engineering. He is presently the Chairman of the Canadian CNC, URSI Commission B, and holds adjunct appointments at the University of Manitoba, and at Queen's University in Kingston.